

with dynamic NMR data obtained in these laboratories.<sup>12</sup>

**Acknowledgment.** The principal authors gratefully acknowledge financial support from the NATO Division of Scientific Affairs and in part the Research Corp. (S.D.W. and J.H.H.).

**Registry No.** 1a, 6069-38-1; 1b, 65173-82-2; 1c, 65173-83-3; 2, 33709-65-8; 3, 7137-86-2.

## References and Notes

- (1) (a) Auburn University. (b) University of Birmingham.
- (2) L. V. Vilkov, L. S. Khaikin, and V. V. Evdokimov, *Zh. Strukt. Khim.*, **10**, 1101 (1969).
- (3) A. H. Cowley, M. J. S. Dewar, D. W. Goodman, and J. R. Schweiger, *J. Am. Chem. Soc.*, **95**, 6506 (1973).
- (4) M. F. Lappert, J. B. Pedley, B. T. Wilkins, O. Stelzer, and E. Unger, *J. Chem. Soc., Dalton Trans.*, 1207 (1975).
- (5) E. Fluck and D. Weber, *Z. Naturforsch. B*, **29**, 603 (1974).
- (6) G. A. Gray and T. A. Albright, *J. Am. Chem. Soc.*, **98**, 3857 (1976).
- (7) A. H. Cowley, D. W. Goodman, N. A. Kuebler, M. Sanchez, and J. G. Verkade, *Inorg. Chem.*, **16**, 854 (1977).
- (8) J. H. Hargis and S. D. Worley, *Inorg. Chem.*, **16**, 1686 (1977).
- (9) J. H. Hargis, S. D. Worley, W. B. Jennings, and M. S. Tolley, *J. Am. Chem. Soc.*, **99**, 8090 (1977).
- (10) L. W. Yarbrough, II, and M. B. Hall, *Inorg. Chem.*, **17**, 2269 (1978).
- (11) A. H. Cowley, R. E. Davis, M. Lattman, M. McKee, and K. Ramadna, submitted for publication; we thank A. H. Cowley for a preprint of this work.
- (12) J. H. Hargis, S. D. Worley, W. B. Jennings, and M. S. Tolley, submitted for publication in *J. Am. Chem. Soc.*
- (13) F. Ramirez, A. S. Gulati, and C. P. Smith, *J. Am. Chem. Soc.*, **89**, 6283 (1967).
- (14) For example, see E. Heilbronner and H. Bock, "The HMO Model and Its Application", Wiley, London, 1976.
- (15) P. A. Bischoff, J. A. Hashmall, E. Heilbronner, and V. Hornung, *Tetrahedron Lett.*, 4025 (1969); E. Heilbronner and K. A. Muszkat, *J. Am. Chem. Soc.*, **92**, 3818 (1970).
- (16) S. F. Nelson and J. M. Buschek, *J. Am. Chem. Soc.*, **96**, 7930 (1974).
- (17) See H. Bock and P. D. Mollere, *J. Chem. Educ.*, **51**, 506 (1974), and references quoted therein.
- (18) S. D. Worley and J. H. Hargis, unpublished results.
- (19) A. H. Cowley, M. Lattman, R. A. Montag, and J. G. Verkade, *Inorg. Chim. Acta*, **25**, L151 (1977).
- (20) Cowley and co-workers (ref 19) have suggested that a similar situation exists for trimethyl phosphite.

Contribution from the Research School of Chemistry,  
The Australian National University, Canberra, ACT, Australia

## Paramagnetic Anisotropy, Average Magnetic Susceptibility, and Electronic Structure of Intermediate-Spin $S = 1$ (5,10,15,20-Tetraphenylporphyrin)iron(II)

PETER D. W. BOYD, DAVID A. BUCKINGHAM, ROBERT F. McMEEKING, and SAMARESH MITRA\*<sup>1</sup>

Received June 25, 1979

Measurements of average magnetic susceptibility and magnetic anisotropy on the single crystals of FeTPP in the 4–300 K temperature range are reported. These results together with the other existing evidence establish an  $S = 1$  spin state for the iron(II) ion in FeTPP. It is shown that the experimental principal susceptibilities cannot be explained over the entire temperature region by a spin Hamiltonian formalism for the  $S = 1$  ground state. A detailed ligand field calculation is presented which gives a satisfactory explanation of the magnetic data. The ligand field calculation indicates a  $d_{z^2}$  orbital lying lowest with  $^3A_2$  as the ground state followed by  $^3E$  and  $^3B$ , in ascending order of energy. The best fit to the data is obtained only in the region where three states come close together.

### Introduction

Iron(II) porphyrins are currently of much interest as they provide a model system to understand the properties of heme proteins.<sup>2</sup> Until recently iron(II) porphyrins were known to exist in either a low-spin ( $S = 0$ ) or a high-spin ( $S = 2$ ) state. No definite evidence of an intermediate-spin state ( $S = 1$ ) was known among iron(II) porphyrins, though there had been speculation on the existence of such an unusual spin state in certain heme proteins.<sup>3</sup> An intermediate-spin state is, however, definitely known to exist in the related iron(II) phthalocyanine, FePc.<sup>4,5</sup>

Magnetic moments of some iron(II) porphyrins have been measured at room temperature, but their high values (4.75–4.85  $\mu_B$ ) have led earlier workers to ascribe them to a high-spin state.<sup>6–8</sup> The first definite suggestion of an intermediate-spin state in iron(II) porphyrins came from the work of Collman et al.<sup>9</sup> on (5,10,15,20-tetraphenylporphyrin)iron(II), FeTPP. They prepared FeTPP by the chromous reduction of FeTPP<sub>2</sub>Cl<sub>2</sub>, which gives a highly crystalline sample.<sup>10</sup> On the basis of detailed molecular structure, room-temperature magnetic moment ( $\approx 4.4 \mu_B$ ), and Mössbauer studies, they suggested an  $S = 1$  spin state for FeTPP. The X-ray crystal structure of FeTPP shows a nearly square-planar geometry around the iron atom, as in FePc, with a very short Fe–N bond favoring strongly an  $S = 1$  spin state.<sup>11</sup> Two recent isotropic proton-shift studies<sup>12,13</sup> also indicate an  $S = 1$  spin state for FeTPP.

Although these studies indicate that the ground state of FeTPP is a spin triplet ( $S = 1$ ), our understanding of the electronic structure of ferrous iron in FeTPP that leads to this situation is still not clear. In particular the origin of the rather high magnetic moment associated with this spin state is still obscure. Speculations about the electron configuration corresponding to the ground state have been made from a consideration of Mössbauer<sup>9</sup> and isotropic proton contact shift<sup>12</sup> measurements, but little information is available about the excited electronic states. Such information may be obtained from studies of the temperature dependence of the principal magnetic susceptibilities<sup>14</sup> of FeTPP. We have therefore measured the average magnetic susceptibility and paramagnetic anisotropy of single crystals of FeTPP between 4.2 and 290 K. These results have been used to deduce the electronic structure of this iron(II) complex.

### Experimental Section

**Preparation of FeTPP.** FeTPP was prepared by the method of Collman et al.<sup>9</sup> All manipulations for the preparations were carried out in an inert atmosphere within a glovebox. Solvents used were deaerated. Crystals large enough for magnetic measurements were grown by seeding the small well-formed purple tetragonal crystals, obtained by the above method. The crystals were chemically analyzed. Anal. Calcd: C, 79.05; H, 4.2; N, 8.4. Found: C, 79.0; H, 4.1; N, 8.7. Their identity was also established by a spectroscopic method and finally by matching the unit cell dimensions by an X-ray method using rotation and Weissenberg photographs.

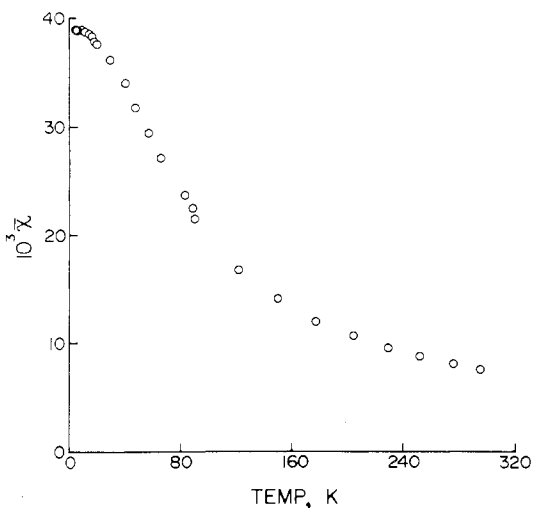


**Figure 1.** Temperature dependence of the average magnetic susceptibility of FeTPP.

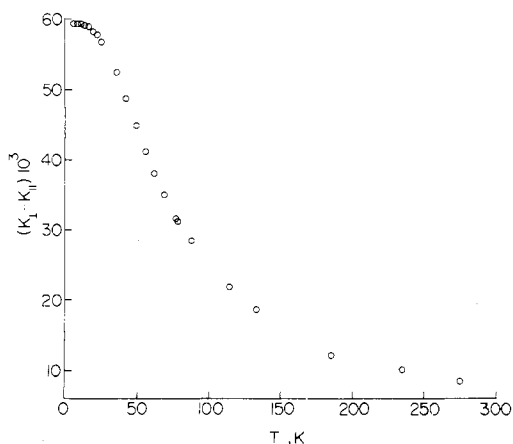


**Figure 2.** Temperature dependence of the molecular anisotropy of FeTPP.

**Magnetic Measurements.** The average magnetic susceptibility of FeTPP was measured on an automatic Oxford Instruments Faraday magnetometer.<sup>15</sup> The system consists of a liquid helium Dewar with superconducting solenoids to provide the main and gradient fields, a variable-temperature insert for sample temperature control, and a Sartorius microbalance for the measurement of force on the sample. A main field of about 10 000 Oe was employed, the gradient field being 1000 Oe/cm. The temperature of the sample was monitored by a carbon resistor and thermocouples; the details of their calibration are described elsewhere.<sup>15</sup>

The magnetic anisotropy was measured by Krishnan's critical couple method<sup>16,17</sup> at field strengths between 850 and 4500 Oe. Quartz fibers approximately 20  $\mu\text{m}$  thick were used and calibrated with respect to the magnetic anisotropy of 1,3,5-triphenylbenzene at room temperature.<sup>18</sup> An Oxford Instruments modular Dewar was used to obtain temperatures between 5 and 300 K. A chromal-Fe(Au) thermocouple was used to measure the temperature. The details of the control of temperature and calibration of the thermocouples are described elsewhere.<sup>15</sup>

For the measurement of the average magnetic susceptibility the polycrystalline sample was packed into an airtight previously calibrated gold bucket Kel-F threaded lid. All the operations of sample grinding and loading into the bucket were done in an inert atmosphere in the glovebox. Similar precautions, as far as practical, were taken during the single-crystal measurement. Measurements on at least three different polycrystalline and single-crystal samples were performed; the results in each case agreed to within  $\pm 1\%$ . The single crystals of FeTPP belong to the tetragonal system<sup>9</sup> and are isomorphous with CuTPP.<sup>19</sup> All the "planar" FeTPP molecules in the unit cell are parallel to the *c* axis of the crystal, and hence the crystal and molecular anisotropies of FeTPP are same. The experimental anisotropies must,

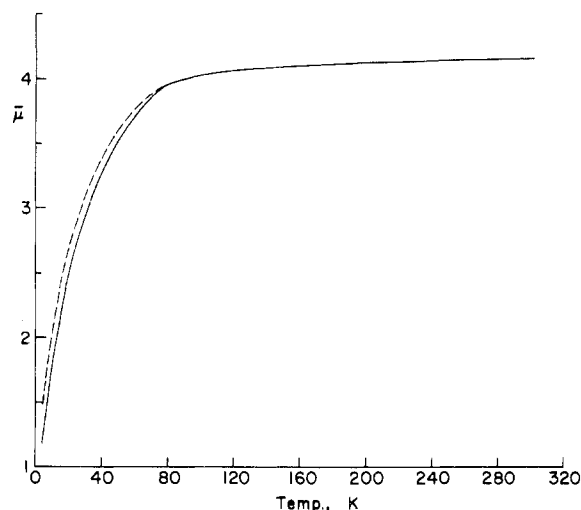


**Figure 3.** Temperature dependence of the average magnetic moment of the polycrystalline samples of FeTPP, one exposed to air (---) and the other not exposed to air (or oxygen) (—).

however, be corrected for the diamagnetic anisotropy of the porphyrin ring. The diamagnetic anisotropy of NiTPP,  $K_{\perp} - K_{\parallel} = 525 \times 10^{-6} \text{ cm}^3/\text{mol}$ , was used for this correction.<sup>20,21</sup> The results of the magnetic measurements shown in Figures 1 and 2 are the corrected values.

The degree of sensitivity of FeTPP to aerial oxidation appears to depend on the method of preparation of FeTPP. Thus Kobayashi and Yanagawa<sup>6</sup> observed that their preparation (which yields an almost amorphous form of FeTPP) is very sensitive to oxidation, a result which we confirm, while the highly crystalline form produced by Collman and Reed appears moderately inert. In solution, of course, FeTPP is very sensitive to oxidation from the air, the end product of this being the  $\mu$ -oxo dimer of iron(III) tetraphenylporphyrin. To determine the effect (if any) of exposure to air on the magnetic properties of FeTPP, we measured the bulk magnetic susceptibility over the entire temperature range of a sample in the normal way, taking all precautions to prevent oxidation, and then removed the sample and ground it in air for several days. The bulk susceptibility of the sample was then remeasured. Figure 3 shows a plot of magnetic moment ( $\bar{\mu}$ ) for both the exposed and pure samples. It is evident that exposure to air in the solid state does not markedly affect the magnetic properties at high temperatures. The slight increase in  $\bar{\mu}$  at lower temperatures indicates that this exposure to air is not producing the  $\mu$ -oxo dimer of Fe<sup>III</sup>TPP and that some small amount of a high-spin iron(II) or iron(III) species is being formed.

## Discussion

The magnetic moment of FeTPP at room temperature is about  $4.2 \mu_B$ , which is close to the value reported by Collman et al. This value is only slightly higher than that reported for the  $S = 1$  FePc ( $\bar{\mu} = 3.9 \mu_B$ ).<sup>4</sup> The present value for FeTPP is, however, quite different from that reported by Kobayashi and Yanagawa<sup>6</sup> ( $\bar{\mu} = 4.75 \mu_B$ ) and Husain and Jones<sup>7</sup> ( $\bar{\mu} = 4.85 \mu_B$ ). The latter two groups have prepared FeTPP by methods different from that of Collman and Reed. We have also studied the magnetic properties of the FeTPP sample as prepared by the method of Kobayashi and Yanagawa and confirm the above difference in the room temperature value, though temperature dependence in both cases is similar.<sup>22</sup> It is not, however, clear at this stage what this difference in the magnetic moment between various methods of preparation represents, as the structure of the Kobayashi preparation is unknown.

The temperature variation of the average magnetic moment of FeTPP bears a close resemblance to that of FePc. The magnetic moment is almost independent of temperature from 300 to 100 K and then decreases, first rather slowly and then sharply, as the temperature decreases further (Figure 3). More characteristic is the near-constant value of  $\bar{\chi}$  below about 10 K (Figure 1). These results are indicative of a large zero-field

splitting of the ground state with a nonmagnetic level lying lowest.

The molecular anisotropy data of FeTPP in Figure 2 show that, as in FePc,  $K_{\perp} > K_{\parallel}$  throughout the temperature range. The parallel and perpendicular subscripts here denote the quantities parallel and perpendicular to the  $c$  axis of the crystal (i.e., the symmetry axis of the molecule). Like  $\bar{\chi}$ , the molecular anisotropy becomes nearly independent of temperature below about 10 K. Recent measurements<sup>23</sup> on FePc show a similar behavior for the molecular anisotropy at very low temperatures. There is close agreement between the value of molecular anisotropy of FeTPP as deduced by Goff et al.<sup>12</sup> from the isotropic proton shift measurement in solution and our directly determined value for the single crystal. The agreement is somewhat unexpected considering that the measurements were performed in the solid state and in solution where the structure of the molecule may be expected to be slightly different, leading to changes in the magnetic anisotropy of FeTPP.

The results presented above together with the information available from molecular structure, Mössbauer, and isotropic proton shift studies confirm that FeTPP is indeed an unusual example of an  $S = 1$  spin state. Our magnetic measurements on a number of other iron(II) porphyrins (e.g., (octaethylporphyrin)iron(II), (deuteroporphyrin dimethyl ester)iron(II)) also indicate an  $S = 1$  spin state.<sup>22</sup> There must be a very large orbital contribution to the magnetic moment in the iron(II) porphyrins to raise the magnetic moment to, say,  $4.2 \mu_B$  for FeTPP from the spin-only value of  $2.83 \mu_B$ . The origin of such a large orbital contribution to the magnetic moment in  $S = 1$  iron(II) systems has been in the past quite enigmatic,<sup>24-26</sup> and no satisfactory explanation has been available. This problem is discussed below during the course of a quantitative analysis of the results on FeTPP, and we attempt an explanation on the basis of the electronic structure of the ferrous ion in a square-planar environment of  $D_4$  symmetry.

**Quantitative Analysis.** The normal method of analyzing data such as that for FeTPP is based on the spin Hamiltonian (SH) formalism where the ground-state properties are described in terms of the properties of an  $S = 1$  state with (in this case axial) zero-field splitting arising from mixing of this state with higher excited states.

This theoretical model has been used in the past for the FePc and other  $S = 1$  iron(II) and cobalt(III) compounds.<sup>4,5,27,28</sup> Following the SH formalism, it is assumed that the ground state of the ferrous ion in FeTPP is an orbitally nondegenerate spin triplet with no close-lying excited states. Spin-orbit coupling partly lifts the spin degeneracy of the ground state into  $M_S = 0$  and  $M_S = \pm 1$  with a separation  $D$ , the zero-field-splitting (ZFS) parameter. Experimental data show that  $M_S = 0$  lies below  $M_S = \pm 1$ .

Expressions 1 and 2 for the principal magnetic susceptibility

$$K_{\parallel} = (2N\beta^2/kT)g_{\parallel}^2(e^d + 2)^{-1} \quad (1)$$

$$K_{\perp} = (2N\beta^2/D)g_{\perp}^2[(e^d - 1)/(e^d + 2)] \quad (2)$$

can then be obtained where  $d = D/kT$ . As  $T \rightarrow 0$ ,  $K_{\parallel} \rightarrow 0$ , and eq 2 becomes

$$K_{\perp} = (2N\beta^2/D)g_{\perp}^2$$

Hence,

$$\bar{\chi}_{T \rightarrow 0} = (4N\beta^2/3D)g_{\perp}^2 = \frac{2}{3}(K_{\perp} - K_{\parallel}) \quad (3)$$

From the  $\bar{\chi}$  and  $K_{\perp} - K_{\parallel}$  data below 10 K, we get

$$g_{\perp}^2 = 0.1139D \quad (4)$$

Substituting for  $g_{\perp}^2$  in eq 2 we get

$$K_{\perp} = 2N\beta^2 \times 0.1139[(e^{D/kT} - 1)/(e^{D/kT} + 2)] \quad (5)$$

Equation 5 has only one parameter,  $D$ , and can be tested

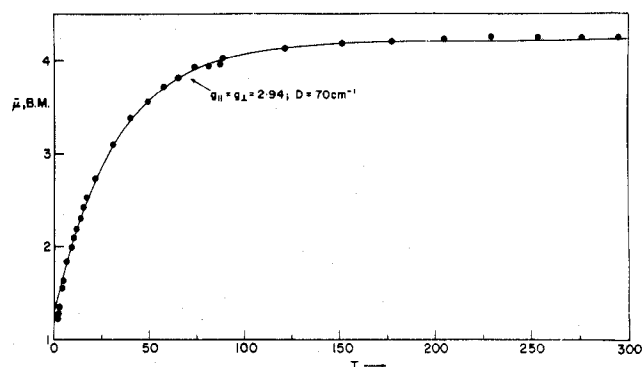


Figure 4. Fit of the average magnetic moment ( $\mu$ ) of FeTPP to the spin Hamiltonian formalism.

against the experimental results of  $K_{\perp}$  obtained by combining the  $K_{\perp} - K_{\parallel}$  and  $\bar{\chi}$  data. The result of such a test is given below:

$T$ , K	$D$ , $\text{cm}^{-1}$	$T$ , K	$D$ , $\text{cm}^{-1}$
10	65.0	90	90.4
20	64.9	200	97.3
30	66.0	270	98.4
40	70.5		

It is obvious that the normal SH model is unable to fit the principal susceptibility data and the paramagnetic anisotropy of FeTPP over the entire temperature range. It is interesting to note here that, when the above model was used to fit the average magnetic moment alone, an excellent fit was found (Figure 4) for  $D = 70 \text{ cm}^{-1}$  and  $g_{\parallel} = g_{\perp} = 2.94$ . This fortuitous agreement essentially reflects the insensitive nature of the average data to theoretical models and cautions against the use of the average magnetic data alone, as is often the practice.<sup>27,28</sup> The principal susceptibilities or magnetic anisotropy provides a very sensitive test for this purpose, as in FeTPP, and has been noted before in a number of cases.<sup>14,29-31</sup>

The failure of the SH model to account for the magnetic data, especially of the principal susceptibility, in FeTPP suggests that there may be one or more low-lying excited states, and the electronic structure of the ferrous ion in FeTPP may be rather complicated. As will be seen, the complete spin Hamiltonian to describe the true electronic ground state of the molecule would have to include a  ${}^3A$ ,  ${}^3E$ , and  ${}^3B$  term leading to a considerable number of spin Hamiltonian parameters. A more satisfying approach would, then, be to use a ligand field model to describe the electronic structure and magnetic properties of the molecule.

**Ligand Field Theory.** The electronic structure of iron(II) complexes in lower than octahedral symmetry has been studied with the ligand field model only recently. König and Schnakig<sup>32</sup> and Kobayashi and Yanagawa<sup>6</sup> have reported some ligand field calculations for  $d^6$  complexes investigating limited areas of ligand field space for potential ground states.<sup>33</sup> However, a detailed investigation of the ground state possible for  $d^6$  complexes in square-planar or five-coordinate geometries is still not available. The introduction of spin-orbit coupling into this model causes extensive mixing of states especially in the "crossover" regions where there may be several close-lying states.

In  $D_4$  symmetry the high-spin ( $S = 2$ ) ground state is formed for the general electronic configuration  $(xy)^2(yz)^1(xz)^1(z^2)^1(x^2 - y^2)^1$  (where no specific orbital energy order is implied). Upon removal of the  $x^2 - y^2$  orbital to higher order energies the changing electron configurations can give rise to a variety of triplet ground states.<sup>32</sup> An investigation of the possible ground states for various electron configurations was made and the consequent magnetic properties for each of these ground state were calculated by using following LF model.

**LF Model.** Ligand field calculations were performed by following a previously described procedure whereby ligand field parameters are related to an effective operator which acts upon the d-electron wave function.<sup>34</sup> The parameterization used was in terms of the one-electron energies of the real d orbitals. Thus for a system of  $D_4$  symmetry there are three parameters representing the relative energies of the  $a_1(z^2)$ ,  $b_2(xy)$ , and  $b_1(x^2 - y^2)$  orbitals to the  $e(xy, yz)$  set. We choose to represent our effective operator in terms of sums of normalized spherical harmonics.<sup>35</sup> Only three coefficients are required for d electrons in  $D_4$  symmetry, the operator having the form<sup>36</sup>

$$\hat{O} = C_{20}Y_2^0 + C_{40}Y_4^0 + C_{44}(Y_4^4 + Y_4^{-4})$$

Evaluation of the coefficients  $C_{20}$ ,  $C_{40}$ , and  $C_{44}$  is possible by using the relations given in Table II of ref 34.

It is convenient to initially express the many-electron wave functions in terms of the  $|J M_J\rangle$  quantization. Here the evaluation of matrix elements with respect to the interelectronic repulsion, spin-orbit coupling, and magnetic moment operators is straightforward. For the normalized spherical harmonic operators  $Y_2^0$ ,  $Y_4^0$ ,  $Y_4^4$ ,  $Y_4^{-4}$  the use of well-established tensor algebra is required and is readily programmed. All reduced matrix elements required in the calculations are given by Neilson and Koster.<sup>37</sup>

A complete  $d^6$  basis set requires the diagonalization of a  $210 \times 210$  matrix and is too large for routine computation. Exclusion of the singlet states is possible in the region of magnetic interest of this work and reduces the basis set to 160. More useful is the symmetry adaption of the basis set which converts the matrix to be diagonalized into five independent blocks corresponding to the irreducible representations of the  $D_4$  group. Here equations similar in form to those given by Griffith<sup>38</sup> for the group  $O^*$  must be applied.<sup>39</sup> Such a symmetry-adapted basis set was used in the calculation of magnetic moments.<sup>40</sup> It consists of subblocks of lengths 23 ( $A_1$ ), 19 ( $A_2$ ), 20 ( $B_1$ ), 20 ( $B_2$ ), and 39 (E). For the ground-state-configuration calculation, where spin-orbit coupling was not included but the complete basis set was used,  $|LSM_L M_S\rangle$  quantization is more appropriate. Accordingly, the basis set was recoupled and  $L$  values were symmetry adapted. Only one spin value need be retained per  $L$  value. Such a procedure generates the subblocks (no  $^5A_2$  occurs).

Figure 5 shows several plots of the ground-state energy boundaries as a function of the three energy separations. In this case the parameters for each diagram are the energies of the  $a_1$  and  $b_2$  orbitals with respect to the  $e$  orbitals for different energies of the  $b_1$  orbital. The interelectronic repulsion parameters  $F_2$  and  $F_4$  have been set to 1000 and 100  $\text{cm}^{-1}$ , respectively. Small variations in  $F_2$  and  $F_4$  do not significantly change the form of the ground-state energy diagrams shown in Figure 5 and accordingly we have used these values in all our calculations.

It can be seen (cf. Figure 5a) that for low values of  $E_{d_{z^2}}$  three spin quintets are possible:  $^5A_1$ ,  $^5E$ , and  $^5B_2$ . As the  $b_1$  orbital moves to higher energy, several triplet states are possible (cf. Figure 5b,c). Of particular interest is the "crossover" region in Figure 5b,c where four and three states, respectively, are nearly coincident, namely,  $^3A_2$ ,  $^3B_2$ ,  $^5A_1$ , and  $^3E$  (shown in b) or  $^3B_2$ ,  $^3A_2$ , and  $^3E$  (shown in c); the latter coincidence is maintained to high energy values of  $b_1$ . Magnetic susceptibilities (calculated by using the van Vleck equation<sup>38</sup>) in the various regions of ligand field parameter space showed that triplet states well isolated from other states such as  $^3A_2$ ,  $^3B_2$ , or  $^3E$  could not give rise to sufficiently high magnetic moments or the correct magnitude for the magnetic anisotropy and in some cases even the correct sign of the anisotropy. But it was found that in the near-"coincidence" region as marked in Figure 5c it was possible to get an increased magnetic moment and correct anisotropies. Figure 6 shows a plot of the low-lying

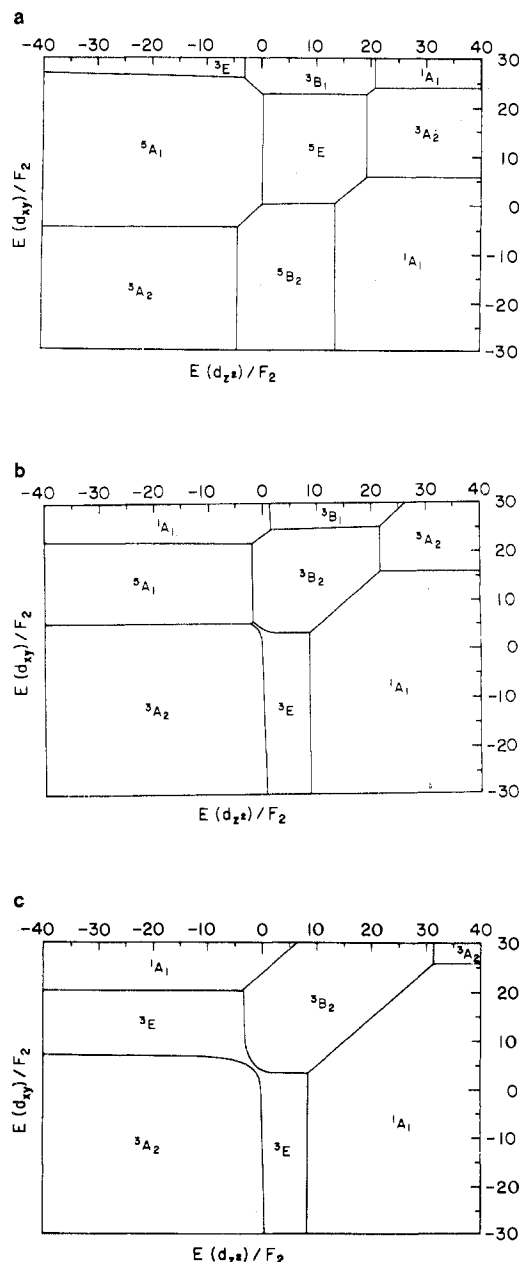


**Figure 5.** Regions of parameter space defining the different ground states for a  $d^6$  electron configuration in  $D_4$  symmetry: (a)  $E(x^2 - y^2) = 15000 \text{ cm}^{-1}$ ,  $E(xz, yz) = 0$ ,  $F_2 = 1000 \text{ cm}^{-1}$ ,  $F_4 = 100 \text{ cm}^{-1}$ ; (b)  $E(x^2 - y^2) = 25000 \text{ cm}^{-1}$ ,  $E(xz, yz) = 0$ ,  $F_2 = 1000 \text{ cm}^{-1}$ ,  $F_4 = 100 \text{ cm}^{-1}$ ; (c)  $E(x^2 - y^2) = 35000 \text{ cm}^{-1}$ ,  $E(xz, yz) = 0$ ,  $F_2 = 1000 \text{ cm}^{-1}$ ,  $F_4 = 100 \text{ cm}^{-1}$ .

states in a section across Figure 5c for  $E_{d_{xy}} = 4000 \text{ cm}^{-1}$ . It can be seen that as we change from  $^3A_2$  to  $^3B_2$  through the  $^3E$  region, these three states become very close together. Figure 7 shows the variation of average magnetic moment ( $\bar{\mu}$ ) at 300 K with the energies of  $d_{z^2}$  orbital for various values of  $E_{d_{xy}}$ . The plot spans the region of near "coincidence"; it can be seen that it is only in this region that the high values of magnetic moments are observed. In other regions the magnetic moments are much too low compared to the experimentally observed value. Of particular relevance is the observation that a magnetic moment as high as  $4.9 \mu_B$  at 300 K can be theoretically obtained for a ground-state triplet ( $S = 1$ ), since such high magnetic moments have previously been taken as diagnostic of an  $S = 2$  spin state.<sup>6,7</sup> Figure 8 shows a similar plot for principal magnetic moments.

Consistent with the above observations, it was found that the magnetic susceptibility and anisotropy could be simulta-

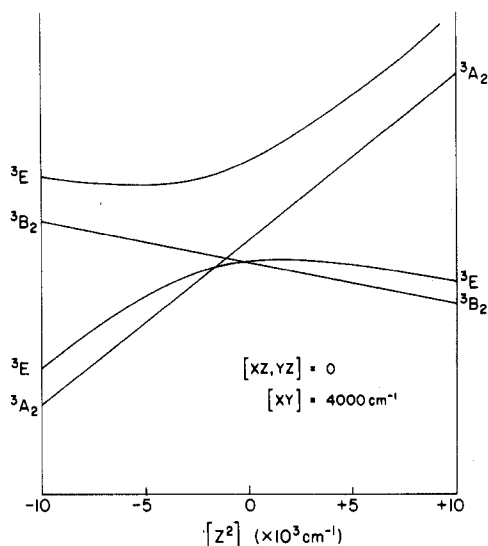


**Figure 6.** Energy level diagram of low-lying states for a  $d^6$  electron configuration in  $D_4$  symmetry as a function of  $E(z^2) = E(xz, yz) = 0$ ,  $E(xy) = 4000$ ,  $E(x^2 - y^2) = 40000$ ,  $F_2 = 1000$ , and  $F_4 = 100$   $\text{cm}^{-1}$ .

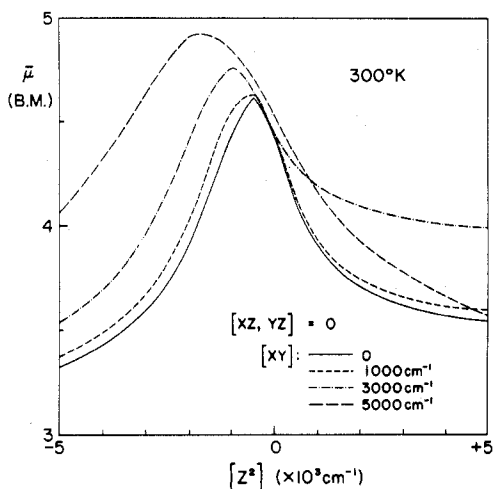


**Figure 7.** Dependence of the average magnetic moment at 300 K on  $E(z^2)$  for various values of  $E(xy)$ .  $\zeta = 380$   $\text{cm}^{-1}$ ,  $E(xz, yz) = 0$ ,  $E(x^2 - y^2) = 40000$   $\text{cm}^{-1}$ .

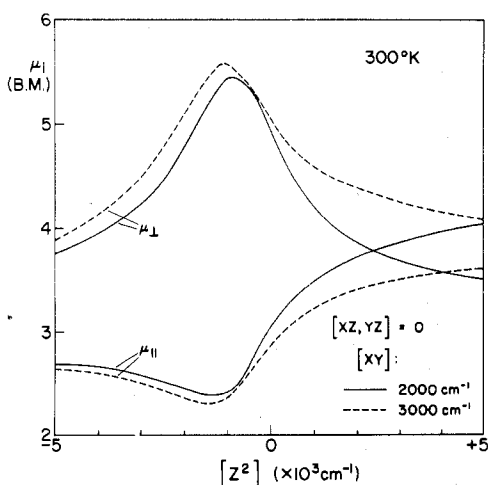


**Figure 8.** Dependence of principal magnetic moments at 300 K on  $E(z^2)$  for different values of  $E(xy)$ .  $E(x^2 - y^2) = 40000$   $\text{cm}^{-1}$ ,  $\zeta = 380$   $\text{cm}^{-1}$ .

neously fitted by using the ligand field model only in the region of near "coincidence". Figures 9 and 10 show the calculated

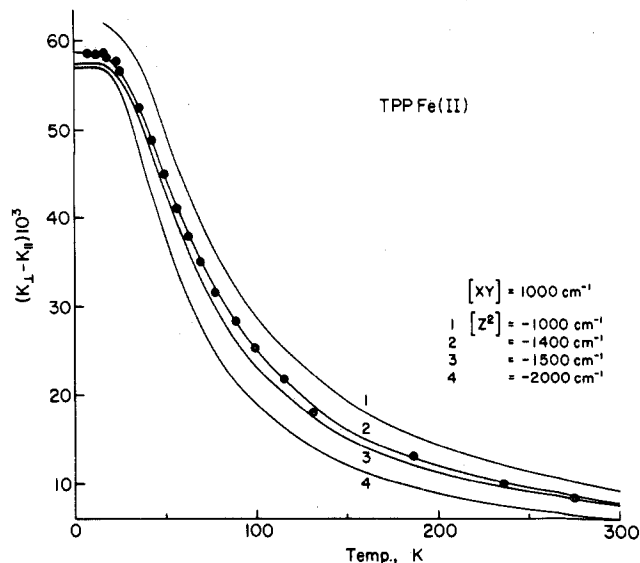


**Figure 9.** Fit of the molecular anisotropy of FeTPP to the ligand field model.  $E(x^2 - y^2) = 40000$   $\text{cm}^{-1}$ ,  $E(xy) = 1000$   $\text{cm}^{-1}$ ,  $E(xz, yz) = 0$ ,  $\zeta = 380$   $\text{cm}^{-1}$ . The effect of the change in  $E(z^2)$  on the fit is shown.

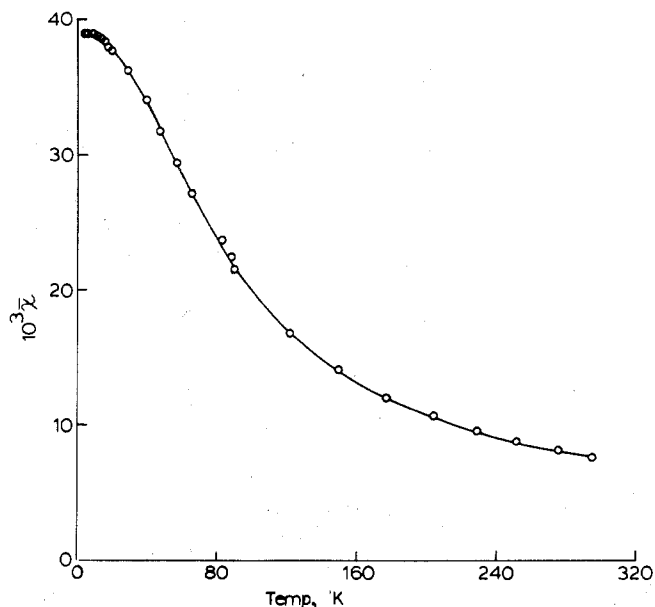


**Figure 10.** Fit of the average magnetic susceptibility of FeTPP to the ligand field model. The values of  $E(x^2 - y^2)$ ,  $E(xy)$ , and  $E(xz, yz)$  are same as in Figure 9.  $E(z^2) = 1425$   $\text{cm}^{-1}$  gives the best fit to the molecular anisotropy (viz. Figure 9).  $\bar{\chi}$  is insensitive to small changes in  $E(z^2)$ , unlike the case for molecular anisotropy.

curves for the best fit to the molecular anisotropy and bulk susceptibility together with calculated curves for slight variations of the one-electron energy levels. A value of  $\zeta = 380$   $\text{cm}^{-1}$  was used in the calculation. The fit is quite good, especially for the molecular anisotropy which is quite sensitive to small variations in the ligand field parameters. Parts a and b of Figure 11 summarize the resulting ordering and schemes for the one-electron energy levels and ground and low-lying states (before spin-orbit coupling), while Figure 11c shows some low-lying spin states of the ferrous ion in FeTPP, as deduced from the present investigation. The important point to note is the considerable mixing of the  ${}^3A_2$ ,  ${}^3E$ , and  ${}^3B_1$  states in the presence of spin-orbit coupling. The ground state is mainly  ${}^3A_2$  and is split by 90  $\text{cm}^{-1}$  (cf. SH model), and there are a number of low-lying excited states. The  ${}^3A_2$  state arises from the electron configuration  $b_2^2 a_1^2 e^2$  and is the configuration favored previously by the Mössbauer and contact shift

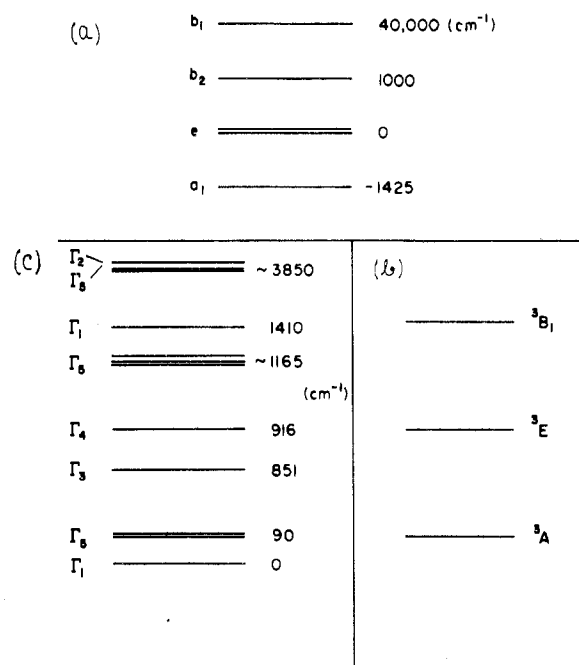


**Figure 11.** Deduced one-electron energies (a), terms (b), and spin states (c) in FeTPP.

studies.<sup>9,12</sup> Alternative configurations to be considered include  $e^4b_2^1a_1^1$ , which gives rise to the  $^3B_1$  state, and  $b_2^2e^3a_1^1$ , which gives rise to the  $^3E$  state. These calculations have shown that both configurations are very close in energy and that the terms arising from each of them are extensively mixed by spin-orbit coupling. These calculations show the danger of simplistic analyses of the data in terms of electron configuration, whereas an accurate description in terms of the spin-orbit-mixed states indicates the difficulty in assigning one particular configuration.

It is worth noting here that the quintet state corresponding to the high-spin ( $S = 2$ ) configuration is found to lie at about  $5000 \text{ cm}^{-1}$  above the ground  $^3A_2$  state but has no effect on the magnetic properties. Removal of the quintet state from our calculation gave identical magnetic properties in the region of ligand field space of present interest.

It is of interest to compare the values of the one-electron energy levels obtained here with those obtained recently for CoTPP from ESR data<sup>42</sup> (cf. Figure 12). The orbital energy scheme sequence is found to be the same although the  $b_2$  orbital is at considerably higher energy than the  $a_1$  orbital in the cobalt case. Also of interest is the comparison of the ground electronic state of FePc and FeTPP. Dale<sup>43</sup> has concluded from Mössbauer measurements on FePc that the most probable ground state for this compound is  $(xy)^2(xz)^1(yz)^2(z^2)^1$ . This is, however, in apparent disagreement with magnetic circular dichroism studies on FePc in dichlorobenzene by Stillman and Thomson,<sup>44</sup> who found that the ground state is  $b_2^2a_1^2e^2$ , the same as we have found for FeTPP. This comparison is interesting in view of the difference in the molecular packing in the solid state in FePc and FeTPP. In the FePc crystals, the planar molecules are stacked in the lattice in such a way that the iron may be considered to have virtually a  $(4 + 2)$  coordination, with the iron atom lying at about  $3.2 \text{ \AA}$  above or below the nitrogen atoms of the adjacent phthalocyanine molecules.<sup>45</sup> This is in contrast to FeTPP where the adjacent molecules are much too far away to have any effect and the iron remains four-coordinated. In the dichlorobenzene solution, the lattice structure is broken and FePc will have a four-coordinate structure, as in FeTPP. The ground-state configuration of FePc and FeTPP in the solid state may not, therefore, be the same, but it is gratifying to find that the

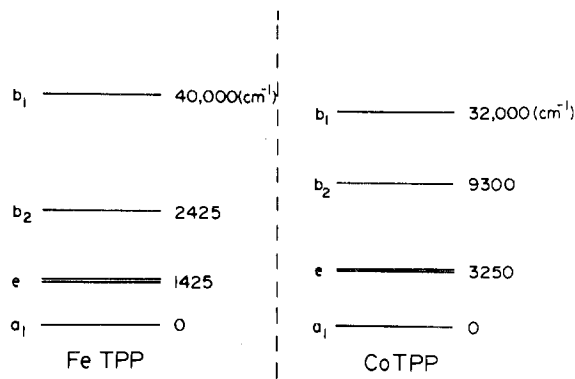


**Figure 12.** Comparison of one-electron energy level schemes for FeTPP and CoTPP.

ground-state configuration of FeTPP and FePc (in solution) are the same.

Finally, we point out the sensitivity of the magnetic properties to the position of the  $a_1$  orbital. Clearly, if even small axial perturbations are made, the magnetic moment and anisotropy are affected significantly. We shall consider this problem later on with regard to other iron(II) porphyrins which we are currently studying.

Recent Mössbauer studies of FeTPP led to a similar conclusion concerning the order of states in this molecule.<sup>46</sup>

**Acknowledgment.** We are very grateful to Christopher Adams and Peter Barlow for their generous help in the experimental work. We also thank Dr. T. B. Rauchfuss for helpful discussions.

**Registry No.** FeTPP, 16591-56-3.

## References and Notes

- (1) To whom correspondence should be addressed at the Tata Institute of Fundamental Research, Chemical Physics Group, Bombay 400 005, India.
- (2) J. P. Collman, *Acc. Chem. Res.*, **10**, 265 (1977).
- (3) J. C. Maxwell and W. S. Caughey, *Biochemistry*, **15**, 388 (1976).
- (4) C. G. Barraclough, R. L. Martin, S. Mitra, and R. C. Sherwood, *J. Chem. Phys.*, **53**, 1643 (1970).
- (5) B. W. Dale, R. J. P. Williams, C. E. Johnson, and T. I. Thorp, *J. Chem. Phys.*, **49**, 3441 (1968).
- (6) H. Kobayashi and Y. Yanagawa, *Bull. Chem. Soc. Jpn.*, **45**, 450 (1972).
- (7) S. M. Husain and J. G. Jones, *Inorg. Nucl. Chem. Lett.*, **10**, 105 (1974).
- (8) D. Brault and M. Rougee, *Biochemistry*, **13**, 4598 (1974).
- (9) J. P. Collman, J. L. Hoard, N. Kim, G. Lang, and C. A. Reed, *J. Am. Chem. Soc.*, **97**, 2676 (1975).
- (10) J. P. Collman and C. A. Reed, *J. Am. Chem. Soc.*, **95**, 2048 (1973).
- (11) J. L. Hoard, M. J. Hamor, T. A. Hamor, and W. S. Caughey, *J. Am. Chem. Soc.*, **87**, 2312 (1965).
- (12) H. Goff, G. N. LaMar, and C. A. Reed, *J. Am. Chem. Soc.*, **99**, 3641 (1977).
- (13) J. Mispetter, M. Momenteau, and J. M. Ihoste, *Mol. Phys.*, **33**, 1715 (1977).
- (14) S. Mitra, *Prog. Inorg. Chem.*, **22**, 309 (1977).
- (15) S. Evans, D. J. Mackey, and R. L. Martin, *J. Chem. Soc., Dalton Trans.*, 1516 (1976).
- (16) K. S. Krishnan and S. Banerji, *Philos. Trans. R. Soc. London, Ser. A*, **234**, 265 (1935).
- (17) S. Mitra, *Transition Met. Chem.*, **7**, 183 (1972).
- (18) K. Lonsdale and K. S. Krishnan, *Proc. R. Soc. London, Ser. A*, **516**, 597 (1936).
- (19) E. B. Fleischer, C. K. Miller, and L. E. Webb, *J. Am. Chem. Soc.*, **86**, 2342 (1964).
- (20) K. S. Murray and R. M. Sheahan, *Aust. J. Chem.*, **28**, 2623 (1975).
- (21) D. V. Behere, V. R. Marathe, and S. Mitra, *J. Am. Chem. Soc.*, **99**, 4149 (1977).
- (22) P. D. W. Boyd, D. A. Buckingham, R. F. McMeeking, T. R. Rausfauss, and S. Mitra, to be submitted for publication.
- (23) R. L. Martin and S. Mitra, to be submitted for publication. We have measured the paramagnetic anisotropy of the FePc single crystals between 300 and 5 K.
- (24) B. N. Figgis, "Introduction to Ligand Fields", Interscience, New York, 1966, Chapter 12.
- (25) L. E. Orgel, *Inst. Int. Chim. Solvay, Cons. Chim. [Rapp. Discuss.]*, 289 (1956).
- (26) A. B. P. Lever, *J. Chem. Soc.*, 1821 (1965).
- (27) E. Konig, G. Ritter, and B. Kanellakopoulos, *J. Chem. Phys.*, **58**, 3001 (1973).

- (28) R. Prins and J. D. W. van Voorst, *Chem. Phys. Lett.*, **1**, 54 (1967).  
 (29) A. K. Gregson and S. Mitra, *Chem. Phys. Lett.*, **3**, 392 (1969).  
 (30) A. K. Gregson and S. Mitra, *Chem. Phys. Lett.*, **3**, 528 (1969).  
 (31) B. N. Figgis, M. Gerloch, and J. Lewis, *J. Chem. Soc. A*, 2028 (1968).  
 (32) E. König and R. Schnakig, *Theor. Chim. Acta*, **30**, 205 (1973).  
 (33) A similar approach has been used by Lever and co-workers for other d-electron configurations and symmetries (J. C. Donini, B. R. Hollebhone, and A. B. P. Lever, *J. Am. Chem. Soc.*, **93**, 6455 (1971)).  
 (34) M. Gerloch and R. F. McMeeking, *J. Chem. Soc., Dalton Trans.*, 2443 (1976).  
 (35) This operator should not be confused with the numerical harmonic Hamiltonian used by Lever and co-workers (*Prog. Inorg. Chem.*, **22**, 225 (1977)). Here each spherical harmonic is "normalized" and the operator is used as described in ref 34.  
 (36) D. M. Brink and G. R. Satchlet, "Angular Momenta", Oxford University Press London, 1968.  
 (37) C. W. Neilson and G. F. Koster, "Spectroscopic Coefficients for the  $p^n$ ,  $d^n$  and  $f^n$  Configurations", MIT Press, Cambridge, Mass., 1963.  
 (38) J. S. Griffith, "The Theory of Transition Metal Ions", Cambridge University Press, New York, N.Y., 1964.  
 (39) Griffith<sup>38</sup> presents equations for the  $O^*$  double group which can be applied to both integral and half-integral  $J$  values. We have written programs which generate equations, in numerical form, for a number of point groups for any required  $J$  value. Only integral  $J$  values are required for even-electron systems. The maximum  $J$  value required for  $d^n$  systems is  $13/2$ .  
 (40) Comparative computational times for the diagonalization of the ligand field matrices, with interelectronic repulsion and nonzero spin-orbit coupling, and calculation of the magnetic properties of symmetry-adapted and non-symmetry-adapted basis sets were performed on the ANU computer center UNIVAC 1100/42.  
 (41) There is in fact a line of fit near the "triple" cross region (see Figure 5c). The spread is, however, not much. One can get perhaps a similar fit by a slightly different choice of electron-repulsion parameters, but any large variation in the parameters may not be possible. What is important is to have a juxtaposition of  $^3A_2$ ,  $^3B_2$ , and  $^3E$  to have  $^3E$  as a mixture of essentially two different configurations.  
 (42) W. C. Lin, *Inorg. Chem.*, **15**, 1114 (1976).  
 (43) B. W. Dale, *Mol. Phys.*, **28**, 503 (1974).  
 (44) M. J. Stillman and A. J. Thomson, *J. Chem. Soc., Faraday Trans. 2*, **70**, 790 (1974).  
 (45) J. M. Robertson, *J. Chem. Soc.*, 615 (1935); 219 (1977).  
 (46) G. Lang, K. Spartalian, C. A. Reed, and J. P. Collman, *J. Chem. Phys.*, **69**, 5424 (1978).

Contribution from the Department of Hydrocarbon Chemistry,  
 Faculty of Engineering, Kyoto University, Kyoto 606, Japan

## An MO Theoretical Study on the Dications of Tetrasulfur, Tetraselenium, and Tetratellurium

KAZUYOSHI TANAKA, TOKIO YAMABE, HIROYUKI TERAMA-E, and KENICHI FUKUI\*

Received February 5, 1979

The electronic structures and the singlet transition energies of the title compounds are studied by using semiempirical INDO-type ASMO-SCF calculations. Localized MO's of each species evaluated from the canonical MO's are also examined. According to the results, these species are all of  $6\pi$  Hückel systems, and their characteristic absorptions at the visible region can be assigned as the highest occupied MO ( $\pi$ )  $\rightarrow$  the lowest unoccupied MO ( $\pi^*$ ) transitions. The electronic structures of  $Te_4^{2+}$  are rather different from those of  $S_4^{2+}$  and  $Se_4^{2+}$  because of the degrees of the contributions from s AO's to the interatomic bonds.

### Introduction

Recent progress in chemistry and physics of the molecular aggregates including chalcogen atoms has had incessant impacts in the field of solid-state science. For instance, polymeric sulfur nitride  $(SN)_x$  is a low-dimensional metallic conductor<sup>1</sup> and even becomes a superconductor at 0.3 K,<sup>2</sup> while amorphous chalcogenide glasses consisting of  $As_2S_3$  or  $As_2Se_3$  have prominent electronic functions available for switching, memory, and imaging devices.<sup>3</sup> Along with the developments of the experimental works, the molecular orbital (MO) theoretical investigations of the electronic structures of these compounds have also been accumulated to reveal their characteristics.<sup>4,5</sup>

Meanwhile, the nature of the chalcogen molecules has gradually become one of the foci of current interest of electronic materials. For example, *cyclo*-octasulfur  $S_8$  and *cyclo*-octaselenium  $Se_8$  being of crown-shaped rings<sup>6</sup> have been studied by UV and X-ray photoemission spectroscopies and compared with the results of the extended-Hückel and the CNDO/S MO treatments.<sup>7</sup> Sulfur-nitrogen compounds also belong to this group, and disulfur dinitride,  $S_2N_2$ , and tetrasulfur tetranitride,  $S_4N_4$ , which are the precursors of  $(SN)_x$ , have been extensively studied from both experimental<sup>8</sup> and theoretical viewpoints.<sup>9</sup>

On the other hand, over these 150 years, it has been known that the elements sulfur, selenium, and tellurium give various intensely colored solutions in strong acids such as sulfuric acid oleum.<sup>10</sup> A series of recent experimental works has succeeded in determining the nature of these colored species.<sup>11</sup> Namely, they are all polyatomic cations of general formula  $X_n^{2+}$  ( $S_4^{2+}$ ,  $S_8^{2+}$ ,  $S_{16}^{2+}$ ,  $Se_4^{2+}$ ,  $Se_8^{2+}$ ,  $Te_4^{2+}$ , and so on), whose characteristic absorption spectra in the near-UV and the visible regions have

all been measured.<sup>11</sup> The geometric structures of these species have been determined by single-crystal X-ray diffraction data of  $S_8^{2+}(AsF_6^-)_2$ ,<sup>12</sup>  $Se_4^{2+}(HS_2O_7^-)_2$ ,<sup>13</sup>  $Se_8^{2+}(AlCl_4^-)_2$ ,<sup>14</sup>  $Te_4^{2+}(AlCl_4^-)_2$ , and  $Te_4^{2+}(Al_2Cl_7^-)_2$ .<sup>15</sup> The structure of  $S_4^{2+}$  has recently been determined from the force constant analysis.<sup>16</sup> No structural data of  $S_{16}^{2+}$  are available at present. The homonuclear groupings of the transition metals are well-known in the "cluster" compounds having ligands attached to the metal cluster, for instance,  $[Mo_6Cl_8]^{4+}$ . In the nonmetal cations like the present  $X_n^{2+}$ , lone pairs of electrons take the place of ligands, which suggests an interesting association with the role of the lone pairs in chalcogenide materials.<sup>3b,5c</sup> The structures of  $X_8^{2+}$  ( $X = S$  or  $Se$ ) cations are those of folded rings with  $C_2$  symmetry,<sup>12,14</sup> and their electronic structures have been investigated on the basis of the MO theoretical treatment by the present authors' group.<sup>17</sup> The geometries of  $X_4^{2+}$  ( $X = S, Se, \text{ or } Te$ ), however, are all of planar four-membered rings,<sup>13,15,16</sup> like  $S_2N_2$ <sup>18</sup> as shown in Figure 1. As to the MO theoretical studies on  $X_4^{2+}$ , there have been only a preliminary work about  $Se_4^{2+}$  on the basis of the Hückel MO method<sup>19</sup> and discussions on the geometric structural differences of  $S_4^{2+}$ ,  $S_4$ , and  $S_4^{2-}$  and on the singlet transition energy of  $S_4^{2+}$  with the use of the SCF- $X\alpha$ -SW method<sup>20</sup> up to now. However, this SCF- $X\alpha$ -SW calculation has given a rather poor result, namely, too small transition energy compared with the observed value,<sup>11</sup> which is reminiscent of an underestimation of the interelectron repulsions in the framework of this calculation. In the present paper, we study the electronic structures of  $S_4^{2+}$ ,  $Se_4^{2+}$ , and  $Te_4^{2+}$  systematically on the basis of the MO theoretical treatment. The localized MO's (LMO's) of the species are also probed in order to obtain a quantitative de-